Development of a Time-Resolved Fluorometric Method for Observing Hybridization in Living Cells Using Fluorescence Resonance Energy Transfer

Akihiko Tsuji, Yoshihiro Sato, Masahiko Hirano, Takayuki Suga, Hiroyuki Koshimoto, Takeshi Taguchi, and Shinji Ohsuka
Laboratory of Molecular Biophotonics, Hamakita 434-8555, Japan

ABSTRACT We previously showed that a specific kind of mRNA (c-fos) was detected in a living cell under a microscope by introducing two fluorescently labeled oligodeoxynucleotides, each labeled with donor or acceptor, into the cytoplasm, making them hybridize to adjacent locations on c-fos mRNA, and taking images of fluorescence resonance energy transfer (FRET) (A. Tsuji, H. Koshimoto, Y. Sato, M. Hirano. Y. Sei-Iida, S. Kondo, and K. Ishibashi, 2000, *Biophys. J.* 78:3260–3274). On the formed hybrid, the distance between donor and acceptor becomes close and FRET occurs. To observe small numbers of mRNA in living cells using this method, it is required that FRET fluorescence of hybrid must be distinguished from fluorescence of excess amounts of non-hybridizing probes and from cell autofluorescence. To meet these requirements, we developed a time-resolved method using acceptor fluorescence decays. When a combination of a donor having longer fluorescence lifetime and an acceptor having shorter lifetime is used, the measured fluorescence decays of acceptors under FRET becomes slower than the acceptor fluorescence decay with direct excitation. A combination of Bodipy493/503 and Cy5 was selected as donor and acceptor. When the formed hybrid had a configuration where the target RNA has no single-strand part between the two fluorophores, the acceptor fluorescence of hybrid had a sufficiently longer delay to detect fluorescence of hybrid in the presence of excess amounts of non-hybridizing probes. Spatial separation of 10–12 bases between two fluorophores on the hybrid is also required. The decay is also much slower than cell autofluorescence, and smaller numbers of hybrid were detected with less interference of cell autofluorescence in the cytoplasm of living cells under a time-resolved fluorescence microscope with a time-gated function equipped camera. The present method will be useful when observing induced expressions of mRNA in living cells.

INTRODUCTION

Fluorescence resonance energy transfer (FRET) has been widely used to detect nucleic acids having specific sequences (Cardullo et al., 1988; Clegg et al., 1993; Sixou et al., 1994). When non-labeled target nucleic acids are detected, two fluorescently labeled oligonucleotides, each labeled with a donor or an acceptor, are hybridized to adjacent locations on the target nucleic acids (Cardullo et al., 1988; Mergny et al., 1994; Sei-Iida et al., 2000). On the formed hybrid, the distance between two fluorophores becomes less than 10 nm and FRET occurs resulting in quenching of donor fluorescence and enhancement of acceptor fluorescence intensity. Because the efficiency of FRET is strongly dependent on the distance between donor and acceptor (inverse of sixth power of the distance), FRET does not occur unless the two fluorescent oligonucleotides hybridize. Therefore, the hybrid formation can be detected in the presence of non-hybridizing fluorescent oligonucleotides by measuring changes in fluorescence spectra or fluorescence decay curves, which is useful under the conditions such as in living cells where non-hybridizing oligonucleotides cannot be washed out. The method using two specific oligonucleotide probes has an additional advantage of high specificity for detecting target nucleic acids when the target nucleic acids are detected in the presence of excess amounts of other kinds of nucleic acids.

We recently demonstrated that the above method can be used to detect specific mRNA in living cells (Tsuji et al., 2000). In the article, we injected the fluorescent oligonucleotide pair probes for a high-accessibility site of c-fos mRNA into the cytoplasm of living Cos7 cells expressing c-fos mRNA. We detected the hybrid formed of the two fluorescent oligonucleotides with c-fos mRNA in the cytoplasm in fluorescence images showing FRET under a conventional fluorescence microscope.

In the above study, to observe FRET in living cells, donor fluorescence images with donor excitation and acceptor fluorescence images with donor excitation were obtained, and the latter image was divided by the former image. In the ratio images, FRET caused by hybrid formation was clearly observed in cells in which more than 10^4 molecules of c-fos mRNA were expressed. Fluorescence images were obtained using a cooled CCD camera as a detector and a Hg lamp as an excitation light source. In these measurements, the detection limit of the number of formed hybrids is determined by the intensity of background light such as cell autofluorescence and fluorescence from non-hybridizing oligonucleotide probes.

Cell autofluorescence is a serious problem for observing small numbers of fluorescence molecules in living cells

Received for publication 24 March 2000 and in final form 10 April 2001.
Address reprint requests to Dr. Akihiko Tsuji, Laboratory of Molecular Biophotonics, 5000 Hirakuchi, Hamakita 434-8555, Japan. Tel.: 81-53-584-0250; 81-53-584-0260; E-mail: tsuji@crl.hpk.co.jp.

0006-3495/01/07/501/15 $2.00

under a microscope. When cell autofluorescence intensity is comparable to or larger than the fluorescence intensity of tagged fluorescence molecules, detection of fluorescence signals becomes very difficult. In case of detecting FRET signal in mRNA imaging described above, cell autofluorescence in donor images is one of the major sources of reducing signal-to-noise ratios for detecting and distinguishing FRET fluorescence. Therefore, it needs to make cell autofluorescence intensity reduce or be distinguished from signal fluorescence in measurements. One approach for overcoming this problem is to use total internal reflection fluorescence microscopy (Axelrod, 1987). Laser light as an excitation source is introduced through the objective under a total reflection condition to illuminate only a small area of interest in cells. Using this method, single fluorescence molecule imaging was performed in solution (Tokunaga et al., 1997) and also in living cells (Sako et al., 2000). Another major background source in FRET measurement is non-hybridizing probes. There are a number of non-hybridizing fluorescently labeled oligonucleotide probes in the cytoplasm, and fluorescence from these probes interferes in detection of FRET signal.

The issue of this article is detection of FRET fluorescence from hybrid in the presence of non-FRET fluorescence caused by an excess amount of non-hybridizing fluorescent oligonucleotide probes and in the presence of cell autofluorescence in living cells under a microscope. Those will be required to detect small numbers of target mRNA in living cells using the two-probe FRET method. As an approach to observe quantitatively FRET signals in living cells under a microscope, we chose a time-resolved method. When fluorescence within a wavelength region is measured under a microscope, it is not possible to distinguish fluorescence due to FRET from fluorescence due to excitation by light absorption. One method to distinguish between FRET fluorescence and non-FRET fluorescence is to use fluorescence decay curves. When FRET occurs, donor fluorescence decay becomes faster due to shortened excited-state lifetime, and measured acceptor fluorescence decay becomes slower due to excitation of acceptors by the interaction with excited donor. In addition, cell autofluorescence has a different decay curve from FRET and non-FRET probe decay curves. In the presence of excess amounts of non-FRET donors, measuring donor decays does not work in FRET detection, because it is difficult to distinguish the shorter fluorescence decay of FRET from among the longer fluorescence decay from non-FRET donors. On the other hand, when a combination of a donor having a longer fluorescence lifetime and an acceptor having a shorter lifetime is used, the measured fluorescence decay of acceptors under FRET with moderate efficiency becomes much slower than the acceptor fluorescence decay with direct excitation (Morrison, 1988). Therefore, measurements of acceptor decay curves will provide good signal-to-noise ratios for distinguishing the acceptor fluorescence from the oligonucleotides hybridizing to the target RNA from among the acceptor fluorescence emitted by non-hybridizing oligonucleotides. An additional reason for using acceptor decays is that cell autofluorescence intensity decreases in the acceptor fluorescence wavelength region due to large separation between excitation wavelength and measurement wavelength.

In this study, we examined combinations of donor and acceptor fluorophores and configurations of formed hybrids for longer delays of acceptor fluorescence when a donor-conjugated oligonucleotide and an acceptor-conjugated oligonucleotide hybridized at locations close to each other on the target RNA. A combination of Bodipy493/503 and Cy5 as donor and acceptor was selected. The acceptor fluorescence under FRET had a sufficiently longer delay for distinguishing FRET fluorescence due to hybrid formation from non-FRET fluorescence when the hybrid had a configuration in which the target RNA has no single-strand part between two fluorophores. Spatial separation of 10–12 bases between the donor and acceptor on the formed hybrid was also required. c-fos RNA was detected specifically in solution in the presence of excess amounts of non-hybridizing fluorescent oligonucleotide probes and other kinds of mRNA. We then constructed a time-resolved fluorescence microscopy equipped with cooled CCD cameras with time-gated function and examined detection of small numbers of hybrids in the cytoplasm of living cells.

MATERIALS AND METHODS

Oligonucleotides

Oligodeoxynucleotides (oligo-DNAs) and Bopdipy493/503-labeled oligo-DNAs were obtained from TAKARA Shuzo (Ohtsu, Japan). Bodipy493/503 (Molecular Probes, Eugene, OR) was conjugated at the 5′ end via TFAc-hexanolaminelinker (Perkin-Elmer Applied Biosystems, Norwalk, CT). Labeling of oligo-DNAs with Cy5 was performed as described previously (Tsuji et al., 2000). Briefly, oligo-DNAs containing Uni-Link AminoModifier (Clontech, Palo Alto, CA) at intermediate positions of the nucleotide sequence or oligo-DNAs containing Amine-VN Phosphoramidite (Clontech) at the 3′ end were obtained from TAKARA Shuzo. The oligo-DNA was mixed with FluoroLink Cy5 Mono Reactive Dye (Amersham Pharmacia Biotech, Arlington Heights, IL) in 0.5 M sodium bicarbonate buffer, pH 9.0, and was applied to a reverse-phased high-performance liquid chromatograph (HPLC) to purify Cy5-labeled oligo-DNA. The labeling yield (molar ratio of Cy5 to oligo-DNA) estimated from absorbance at 260 nm and at 650 nm was 0.9–1.0. The oligo-DNAs were dissolved in diethyl pyrocarbonate (DEPC)-treated water.

We used a part of a multicloning site as the target sequence. The sequences of target DNAs, donor probes, and acceptor probes are shown in Table 1. For hybrid formations of double-strand configurations (see Results and Discussion), the target DNA was 33-mer. The donor probe was complementary to the 5′-end half of the target and was labeled with Bodipy493/503 at the 5′ end. The acceptor probes were complementary to the 3′-end half of the target DNA, and Cy5 was conjugated at various positions of the nucleotides. For hybrid formations containing single-strand configurations, the donor probe was complementary to the 5′-end part of the target and was labeled with Bodipy493/503 at the 5′ end. The acceptor probe was complementary to the 3′-end part of the target DNA and was labeled with Cy5 at the 3′ end.

TABLE 1 Sequences of target DNAs, donor probes, and acceptor probes

	Targets and probes	Sequence	*n*
Double-strand configurations			
	Target	5′-GGGTTAATTGCGCGCTGTAATCATGGTCATAGC-3′	
	Donor probe	3′-CCCAATTAACGCGCGA-(Bodipy493/503)-5′	
	Acceptor probe	3′-CATT(Cy5)GTACCAGTATCG-5′	4
		3′-CATTAGTA(Cy5)CAGTATCG-5′	8
		3′-CATTAGTACCAG(Cy5)ATCG-5′	12
		3′-CATTAGTACCAGTA(Cy5)CG-5′	14
Single-strand configurations			
	Target	5′-GGGTTAATTGCGCGCTTGGCAAAAAAAAAAAAAAAAGTAATCATGGTCATAGC-3′	20
		5′-GGGTTAATTGCGCGCTTGGCAAAAAAAAAAAAGTAATCATGGTCATAGC-3′	15
		5′-GGGTTAATTGCGCGCTTGGCAAAAAAAAAGTAATCATGGTCATAGC-3′	12
		5′-GGGTTAATTGCGCGCTTGGCAAAAGTAATCATGGTCATAGC-3′	8
		5′-GGGTTAATTGCGCGCTTGGCGTAATCATGGTCATAGC-3′	4
	Donor probe	3′-CCCAATTAACGCGCGA-(Bodipy493/503)-5′	
	Acceptor probe	3′-(Cy5)-CATTAGTACCAGTATCG-5′	

In the experiments for detecting human c-fos RNA, the 657–696 site of c-fos mRNA was used as a target sequence (Tsuji et al., 2000). The 40-mer target sequence was 5′-GCGGAGACAGACCAACTAGAAGATGAGA-AGTCTGCTTTGC-3′. The donor probe was 5′-Bodipy493/503-TCTAGTTGGTCTGTCTCCGC-3′ and the acceptor probe was 5′-GCAAAGC(Cy5)GACTTCTCATCT-3′.

HPLC

A total of 40 pmol of Bodipy493/503-labeled oligo-DNA and 40 pmol of Cy5-labeled oligo-DNA were mixed with 40 pmol of the target oligo-DNA in 10 μl of 10 mM Tris-HCl, 140 mM NaCl, pH 7.4, and incubated for 5 min at room temperature. This mixture solution was applied to an ion-exchange HPLC to separate the hybrid and free fluorescent oligo-DNAs. The HPLC was performed using a TSK-GEL DEAE-NPR column (Tosoh, Tokyo, Japan) with a NaCl gradient in 20 mM Tris-HCl, pH 9.5 at 25°C. The NaCl concentration gradient was as follows: 0–2 min, 25–45%; 2–12 min, 45–55%; 12–13 min, 55–100%. The flow rate was 1 ml/min. Elution was monitored with absorption at 260 nm and with a fluorescence intensity at 650 nm excited at 475 nm. In the chromatograph, two major peaks appeared. The peak, which appeared at 5 min, showed only 260-nm absorption and little fluorescence, and the peak at 7–9 min showed 260-nm absorption and strong fluorescence. The free probes were eluted at 5 min, and the hybrid was eluted at 7–9 min. The hybrid fractions were recovered, and fluorescence spectra and fluorescence decay curves were measured.

Measurements of fluorescence spectra and decay curves

Fluorescence spectra were measured using HITACHI F-4500 fluorescence spectrophotometer with excitation at 490 nm.

Fluorescence decay curves were measured using a picosecond fluorescence measurement system (Hamamatsu C4780, Itamamatsu, Japan) which utilized a streak scope (Hamamatsu C4334) as a detector, coupled with a pulsed laser. The excitation light pulses (485 nm) were generated by a frequency doubler (a lithium tri-borate crystal) and pulse selector (3980, Spectra Physics) for the light from a mode-locked Ti:Sapphire laser (Tsunami, Spectra Physics, Mountain View, CA) pumped by an argon ion laser (2080, Spectra Physics). The pulse width was less than 2 ps, and its repetition rate was 2 MHz. For measurements of decay curves of Bodipy493/503, the measured wavelength region was set up for 510–560 nm. For measurements of Cy5 fluorescence, the wavelength region was 650–700 nm. The sweep time range was 50 ns. Each decay curve was obtained with 10^9 to 10^{10} pulse counts (count period was 20–30 min).

Time-resolved measurements of Cy5 fluorescence were also performed using gated microchannel plate photomultiplier tubes (R5916U, Hamamatsu) as detectors. A sample cell was placed between two gated microchannel-plate-photomultipliers (MCP-PMT), and the measurements were carried out in a T-format. Excitation light pulses from a mode-locked Ti:sapphire laser with a frequency doubler and pulse selector described above (Spectra Physics) were focused on the sample cell at a right angle to the detection axis. Fluorescence photons were incident on both gated MCP-PMTs through identical optical bandpass filters (Asahi Spectra Co., Tokyo, Japan) possessing a center wavelength of 660 nm and a half-bandwidth of 50 nm. A pulse generator (HP 8110A, Hewlett Packard) synchronized with the laser pulses provided gate pulses with typically a 3-ns width and different delays, and the two gated MCP-PMTs detected fluorescence photons in different time windows on the fluorescence decay. Output pulses from the gated MCP-PMTs were amplified by a fast amplifier and fed to a discriminator (FTA 820A and model 935, respectively, Perkin Elmer, ORTEC, Oak Ridge, TN). A quad counter (model 974, Perkin Elmer, ORTEC) counted laser pulses and the detected fluorescence photons in the two time windows. The time generator and the quad counter were regulated by a PC through a General Purpose Interface Bus. Fluorescence photons in the time windows were counted for 2×10^6 pulses (counting time was 1 s) for each measurement. The program for controlling the delays and width of the gating pulses and data transfer from the quad counter was written in LabVIEW (National Instruments, Austin, TX).

Estimation of donor fluorescence decay curves

Fluorescence decay curves of donor (Bodipy493/503) were made using the formula below, which describes decay curves under conditions where distances between the donor and acceptor are distributed (Grinvald et al., 1972; Eis and Lakowicz, 1993; Parkhurst and Parkhurst, 1995).

$$I_d(t) = A \exp(-t/\tau_d(r)),$$

where

$$\tau_d(r) = \tau_0 (1 - E) = \tau_0(1 - 1)/(1 + (P(r)/R_0)^6),$$

where $I_d(t)$ is intensity of donor fluorescence at time t after excitation, $\tau_d(r)$ is fluorescence lifetime of a donor in the presence of an acceptor at a distance r from the donor, τ_0 is fluorescence lifetime of donor in the

absence of an acceptor, E is efficiency of FRET, R_0 is Forster distance for a combination of donor and acceptor, $P(r)$ is distance-distribution function of the donor and acceptor, and A is the normalization factor.

For distribution of donor-acceptor distances, we used a gaussian function (Eis and Lakowicz, 1993; Parkhurst and Parkhurst, 1995).

$$P(r) = Z \exp(-(r - r_0)^2/2\sigma^2),$$

where r_0 is average distance of donor and acceptor, σ is standard deviation from the average distance, and Z is the normalization factor.

Estimation of signal-to-noise ratios for distinguishing two fluorescence decay curves

The signal-to-noise ratios for distinguishing acceptor decay curves of the hybrid from acceptor decay curves of the non-hybridizing fluorescent oligonucleotides were estimated as described in Soper et al. (1995).

A parameter representing fluorescence decay rate was set as follows:

$$\tau = -\Delta t/\ln(D_1/D_0),$$

where D_0 is fluorescence intensity during 3–5 ns, D_1 is fluorescence intensity during 5–7 ns, and $\Delta t = 2$ ns.

The standard deviation of the measured value (σ) was calculated for each acceptor fluorescence decay curve using the equations below.

$$\sigma = \tau \times (1/D_0 + 1/D_1)^{1/2}/(-\ln(D_1/D_0))$$

The difference in decay rates between the two decay curves ($\Delta\tau = \tau_h - \tau_p$; the subscripts h and p denote the decay curves of hybrid and probes, respectively) was divided by the sum of the standard deviation of measurements ($\sigma_{\Delta\tau} = (\sigma_h^2 + \sigma_p^2)$). These values ($\Delta\tau/\sigma_{\Delta\tau}$) were used as signal-to-noise ratios for distinguishing the two decay curves.

Preparation of c-fos RNA

Human c-fos RNA was prepared as described in Tsuji et al. (2000). The pSPT plasmid containing human c-fos cDNA (pSPT-cfos) obtained from RIKEN Gene-Bank was treated with *Eco*RI to cut off the c-fos DNA (2.1 kb), and the c-fos DNA fragment was inserted into the *Eco*RI site on pBluescriptII KS(+) (Strategene, La Jolla, CA). The plasmid containing c-fos DNA (pBluescript-cfos) was treated with *Sma*I to produce a linearized plasmid and used as a template for in vitro transcription reactions driven by T3 promoter to synthesize c-fos RNA. In vitro transcription reactions were performed using T3 MEGAscript kit (Ambion, Austin, TX)

Preparation of polyA RNA from NIH/3T3 cells

NIH/3T3 cells were cultured with a minimum essential medium supplemented with 10% fetal calf serum in 5% CO_2 at 37°C. Total RNA was extracted from 5×10^7 cells using QuickPrep total RNA extraction kit (Amersham Pharmacia Biotech). Polyadenylated (polyA) RNA was purified using mRNA purification kit (Amersham Pharmacia Biotech).

Microscopy

A block diagram of the time-resolved fluorescence microscope is shown in Fig. 6. The excitation light pulses (460 nm, 150-fs of pulse width, 1 MHz) were generated by a pulse picker (9200, Coherent, Santa Clara, CA) and through a barium β borate crystal for the light from a mode-locked Ti:sapphire laser (Mira900, Coherent) pumped by an argon ion laser (Innova, Coherent). The pulsed light was introduced into an inverted fluorescence microscope (TME-300, Nikon) through an objective (×40/NA = 0.85, Fluor, Nikon). Using a beam expander, the spot width was expanded for illuminating a whole cell on the microscope stage (The diameter of the spot on the stage was ~20 μm when the ×40 objective was used.). Fluorescence from cells was split two ways using a half-mirror after passing a dichroic mirror (550DCLP02, Omega Optical) and a bandpass filter for Cy5 (660DF50, Omega Optical), and each was led to a cooled CCD camera (C4880, Hamamatsu) coupled with an image intensifier with time-gate function (V6561GU1M, Hamamatsu). The obtained fluorescence images were fed to an image analyzer (ARGUS-50, Hamamatsu). Gated timing for measurements in two cameras was triggered from the pulse picker to synchronize it with the laser pulse, and gate pulses for cameras were generated by a delay generator (model DG535, Stanford Research Systems, Sunnyvale, CA). A time-gate window for the first camera was set at one time position on a decay curve and that for the second camera was set at another time position. The ratio value of fluorescence intensity in the two time windows represents the decay rate. Two fluorescence images were acquired using the two cameras. After subtraction of background in each image, the image in the second camera was divided by the image in the first camera to obtain a ratio image.

The conventional epi-fluorescence microscope setting is described in Tsuji et al. (2000). A Hg lamp was used as an excitation light source, and fluorescence images were obtained by a cooled CCD camera (C4880, Hamamatsu). For FRET imaging, donor fluorescence images with donor excitation (DD) and acceptor fluorescence images with donor excitation (DA) were measured, and the ratio images (DA/DD) were obtained.

Microinjection experiments

Hela cells were cultured with Dulbecco's modified Eagle's medium supplemented with 10% fetal calf serum, and various concentrations of probe solutions or hybrid solutions were injected into the cytoplasm of cells. Donor probe was Bodipy493/503-labeled 20-mer DNA for the 657–676 site of human c-fos mRNA. Acceptor probe was Cy5-labeled 20-mer DNA for the 677–696 site of c-fos mRNA. In conventional microscope experiments, the acceptor probe was used in which Cy5 was conjugated at the position between 4 and 5 nucleotides from the 3′ end. In time-resolved microscope experiments, Cy5 was conjugated at the position between 12 and 13 nucleotides from the 3′ end in the acceptor probe. On the formed hybrids, the number of nucleotides separating donor and acceptor was 4 for conventional microscope experiments and 12 for time-resolved microscope experiments. Donor and acceptor probes each were bound to streptavidin to keep them from passing through nuclear pores (Tsuji et al., 2000). A 40-mer DNA having a sequence of the 657–696 site of c-fos mRNA was used as a target nucleic acid. Probe solutions were a 1:1 mixture of donor probe and acceptor probe in PBS. Hybrid solutions were a 1:1:1 mixture (molar ratio) of donor probe, acceptor probe, and target DNA. Microinjection was performed using a micromanipulator (model 5171, Eppendorf) and a transjector (model 5246 Plus/Basic, Eppendorf), and fluorescence ratio images of the cells were obtained in the time-resolved microscope or in the conventional microscope. Fluorescence images were obtained at 5 min after injection. Excitation lights were attenuated through neutral density filters to avoid photobleaching of fluorophores within cells. Image acquisition times were 4 s in DD and DA images in the conventional microscope and 4 s in the time-resolved microscope.

RESULTS AND DISCUSSION

Selection of combinations of donor and acceptor

We measured fluorescence decay curves of various fluorophores conjugated to oligonucleotides including Bodipy-derivatives, fluorescein-derivatives, rhodamine-derivatives, and cyanine-derivatives. Fluorescence lifetimes of these fluorophores were ~7 ns for Bodipy, 4 ns for fluorescein,

1–4 ns for rhodamine, and less than 1 ns for cyanine. For longer delays of acceptor fluorescence in FRET, it is required that the fluorescence lifetime of donor is longer than the lifetime of acceptor, and a larger difference in lifetimes between donor and acceptor is more desirable. We selected a combination of Bodipy-derivatives and cyanine-derivatives as a donor and an acceptor. An additional factor for good distinction of acceptor fluorescence due to FRET from other fluorescence in measurements of decay curves in the wavelength region of acceptor fluorescence is contamination of donor fluorescence. The fluorescence decay of donor in the absence of acceptor is slow. Also, even in the presence of acceptor, the donor decay is relatively slower than the acceptor decay except in cases where FRET efficiency is exceedingly high. Therefore, the presence of donor fluorescence in the wavelength region of acceptor fluorescence reduces signal-to-noise ratios for detecting the acceptor fluorescence due to FRET. It is desirable to use combinations of donor and acceptor in which the acceptor fluorescence is completely separated from the donor fluorescence in wavelength. We selected a combination of Bodipy493/503 and Cy5 for use in the experiments below. In this combination, the spectral overlap between the fluorescence spectrum of donor (Bodipy493/503) and the absorption spectrum of acceptor (Cy5) is relatively small (R_0, Forster distance, is 42 Å). However, FRET occurs efficiently on the formed hybrids because the distance between two fluorophores on the formed hybrid becomes very close. (Fig. 1; also see Tsuji et al., 2000). Another advantage of this combination is the low excitation efficiency of Cy5 at the excitation wavelength for Bodipy493/503 (490 nm).

Fluorescence decay curves in hybrids

First, we measured fluorescence spectra and fluorescence decay curves in the hybrids. We examined two types of hybrid configurations (Fig. 1). In one type, the donor and acceptor fluorescent oligo-DNA hybridized to the target DNA adjacently, which made the hybrid having a double strand between two fluorophores. In another type, two fluorescent oligo-DNAs, either of which was labeled at the 5′ end or the 3′ end, were used and the formed hybrid had a single strand between the two nucleotides conjugating to the fluorophore. We obtained hybrids where two fluorophores were separated by n nucleotides ($4 \leq n \leq 20$) in the single-strand configuration or in the double-strand configuration. A 17-mer Bodipy493/503-labeled oligodeoxynucleotide, a 16-mer Cy5-labeled oligodeoxynucleotide, and a target DNA (33–53-mer) were mixed in solution, and the formed hybrid was purified by HPLC.

Fig. 1, *A* and *D*, shows the fluorescence spectra of the hybrids. In all hybrids examined, quenching of Bodipy493/503 fluorescence and enhancement of Cy5 fluorescence were observed, indicating occurrence of FRET. FRET efficiency (E) was obtained from quenching of Bodipy493/503 fluorescence in the spectrum, and the average distance (r) between two fluorophores on the hybrid was estimated according to $E = 1/(1 + (r/R_0)^6)$, where the R_0 used was 42 Å, assuming a free rotation of fluorophores ($\kappa^2 = 2/3$) (Table 2). As previously reported (Tsuji et al., 2000), in the double-strand configurations, FRET efficiency increased as the number of nucleotides (n) separating two fluorophores on the hybrid became smaller from $n = 14$ to $n = 4$. This was caused by making the average distance between two fluorophores on the hybrid closer in response to the number of (n). In the single-strand configurations, similar results were obtained. Comparing the spectra in the double-strand configurations with the spectra in the single-strand configurations showed that FRET efficiency was higher in the single strand than in the double strand for the same number of (n) (Table 2). Because the single-strand part on the formed hybrid is structurally flexible, the hybrid structure will fluctuate over wider distances. This will cause closer average distances between two fluorophores, which increases FRET efficiency.

Fig. 1, *B* and *E*, shows fluorescence decay curves of Bodipy493/503 (510–560 nm) in the double-strand configuration (Fig. 1 *B*) and in the single-strand configuration (Fig. 1 *E*). Fig. 1, *C* and *F*, shows fluorescence decay curves of Cy5 (650–700 nm) in the double strand (Fig. 1 *C*) and in the single strand (Fig. 1 *F*). Bodipy493/503 fluorescence in the absence of Cy5 showed almost a single exponential decay, and the lifetime was 7.2 ns. Cy5 fluorescence in the absence of Bodipy493/503 also showed a single exponential decay, and the lifetime was 1.0 ns. On the hybrid formed of Bodipy493/503-labeled oligo-DNA and Cy5-labeled oligo-DNA with the target DNA, the decays of Bodipy493/503 became faster than the decay in the absence of Cy5-labeled oligo-DNA in all types of hybrids examined. Decay curves of Cy5 on the hybrids became slower. As the number of nucleotides separating two fluorophores on the hybrid decreased, changes in decay curves became larger, which was caused by higher FRET efficiency. These changes were consistent with changes in the fluorescence spectra.

The decay curves of Bodipy493/503 showed large discrepancies between the single-strand hybrid configurations and the double-strand hybrid configurations. In hybrids of double-strand configurations, the fluorescence decayed approximately single exponentially except in the case of $n = 4$. On the other hand, fluorescence decays in single-strand configurations showed large discrepancies from the single exponential. We have interpreted that the differences in decay curves between the single-strand configurations and the double-strand configurations were caused by differences in the distributed width of distances between the donor and acceptor on the formed hybrid. When the distance between the donor and acceptor is fixed, the donor fluorescence under FRET shows single exponential decay. However, in most cases the distance between the donor and acceptor fluctuates in solution. The donor fluorescence decay curves

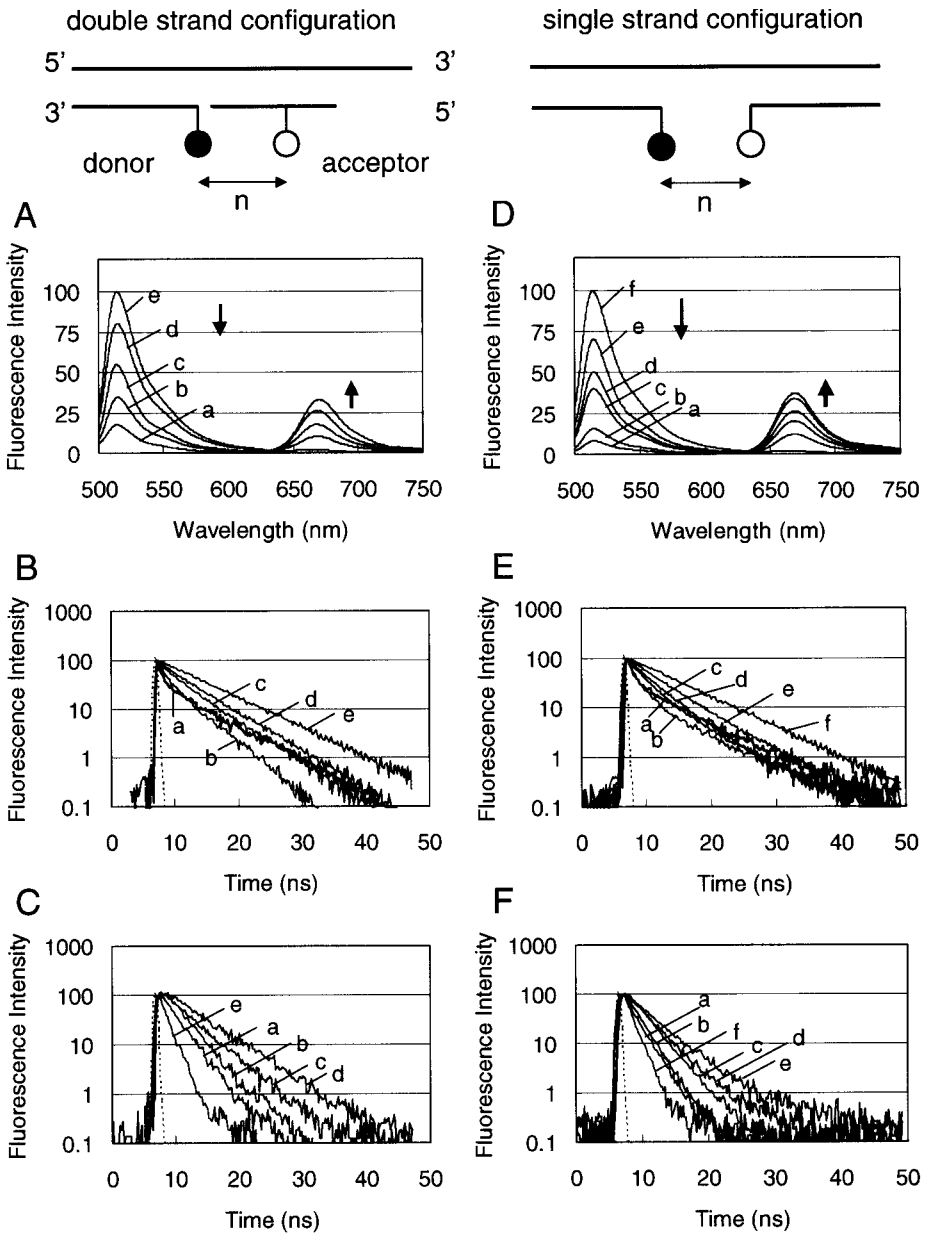

FIGURE 1 Fluorescence spectra and decay curves of hybrids. Two types of configuration of hybrids were prepared. One type of hybrid was a double strand between the two nucleotides conjugating the fluorophore (*left*, *A–C*), and another type was a single strand (*right*, *D–F*). *n*, number of nucleotides separating two fluorophores on the hybrid. (*A*) Fluorescence spectra of double-strand configuration hybrids (these are a repeat of experiments described in Tsuji et al., 2000; $n = 4$ (*a*), 8 (*b*), 12 (*c*), and 14 (*d*); *e*, pair probe solution. (*B*) Fluorescence decay curves of Bodipy493/503 (510–560 nm); $n = 4$ (*a*, *bold line*), 8 (*b*), 12 (*c*), and 14 (*d*); *e*, donor probe. The laser pulse measured by the streak scope is also shown as a broken line. The actual width of the pulses was less than 2 ps. (*C*) Fluorescence decay curves of Cy5 (650–700 nm); $n = 4$ (*a*), 8 (*b*), 12 (*c*), and 14 (*d*); *e*, acceptor probe. (*D*) Fluorescence spectra of single-strand hybrid configuration hybrids; $n = 4$ (*a*), 8 (b), 12 (*c*), 15 (*d*), and 20 (*e*); *f*, pair probe solution. (*E*) Fluorescence decay curves of Bodipy493/503; $n = 4$ (*a*, *bold line*), 8 (*b*), 12 (*c*), 15 (*d*), and 20 (*e*); *f*, donor probe. (*F*) Fluorescence decay curves of Cy5; $n = 4$ (a), 8 (*b*), 12 (*c*), 15 (*d*), and 20 (*e*); *f*, acceptor probe.

vary in response to the width and mode of the fluctuation in donor-acceptor distance (Grinvald et al., 1972; Haran et al., 1992; Eis and Lakowicz, 1993; Parkhurst and Parkhurst, 1995).

Although a detailed analysis of decay curves to elucidate dynamic fluctuations of hybrid structures is not the focus in this article, we performed some analysis of our experimental results (Fig. 1) according to the consideration above. Fluorescence decay curves of Bodipy493/503 were estimated under conditions where the distance between Bodipy493/503 and Cy5 on the formed hybrid fluctuated and the distribution was described as Gaussian. For each hybrid in

TABLE 2 Analysis of fluorescence spectra and decay curves of hybrids

Configuration between two fluorophores on the hybrid	n	E	r (Å)	σ (Å)
Double strand	4	0.83	32.2	ND
Double strand	8	0.65	37.9	4
Double strand	12	0.45	43.4	4
Double strand	14	0.20	52.9	4
Single strand	4	0.92	27.9	ND
Single strand	8	0.84	32.3	ND
Single strand	12	0.60	39.3	12.5
Single strand	15	0.50	42.3	10
Single strand	20	0.30	48.5	15

Analysis of fluorescence spectra and decay curves of the hybrids shown in Fig. 1 is presented. Measurements and analysis of fluorescence spectra in the double-strand configurations were a repeat of experiments described in Tsuji et al., (2000). n, number of nucleotides separating two fluorophores on the hybrid; E, efficiency of FRET estimated from quenching of Bodipy493/503 fluorescence in the spectra; r, average distance between the donor and acceptor on the hybrid, estimated according to $E = 1/(1 + (r/R_0)^6)$ (42 Å of R_0 value (Forster distance) was used for the combination of Bodipy493/503 and Cy5); σ, standard deviation of distance-distribution used for estimations of Bodipy493/503 fluorescence decay curve, which had a good fit with the measured decay curves. Distance-distributions of the donor and acceptor were postulated as Gaussian functions. ND, not determined.

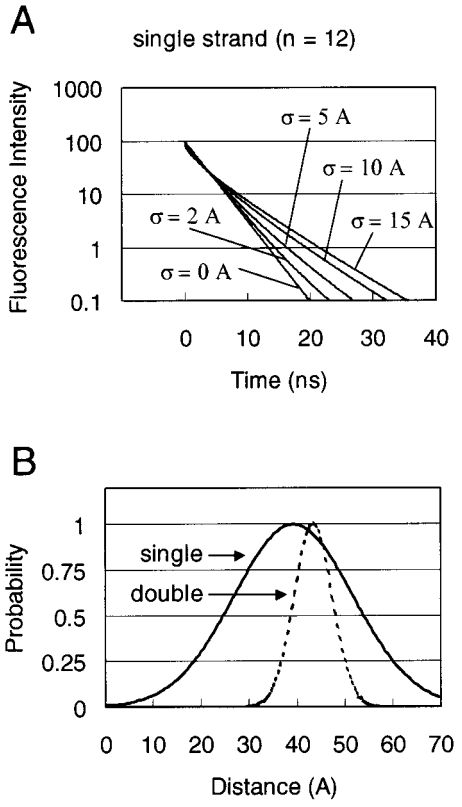

FIGURE 2 Distance-distribution of donor and acceptor on hybrids. (*A*) Effect of the distance-distribution on Bodipy493/503 decay curves. Bodipy493/503 decay curves were calculated in the single-strand configuration hybrid where 12 nucleotides separated two fluorophores and the distance-distributions of donor and acceptor were described as the Gaussian (see text). The width of the distribution (standard deviation σ) varied. (*B*) The standard deviation values showing a good fit of calculated decay curves with the measured decay curves were obtained (see text, Table 2). The distance-distributions of the donor and acceptor were presented for the hybrids of the single-strand configuration and of the double-strand configuration. Twelve nucleotides separated two fluorophores on the hybrids ($n = 12$).

the single- or the double-strand configuration where two fluorophores are separated by n nucleotides, fluorescence decay curves of Bodipy493/503 on the hybrid were calculated according to the formula representing the donor decay curves under Gaussian distributions of the donor and acceptor (see Materials and Methods). In calculations of decay curves, standard deviation values for the distance-distribution varied. Fig. 2 *A* is an example showing effects of the width of distance-distributions on the decay curves. These decay curves were made using the parameter values for the single-strand hybrid configuration in which 12 nucleotides separated two fluorophores (the average distance r was 39.3 Å, Table 2). The decay curve was the single exponential when the standard deviation for the distribution (σ) was zero. As distributions had wider ranges, the curves showed larger discrepancies from the single-exponential decay and throughout the slower decays in the latter part of the decay curve.

The calculated decay curves were compared with the measured curves (Grinvald et al., 1972), and the standard deviation values (σ) for the good fitted results were determined (Table 2). The calculated decay curves with narrow distance-distributions ($\sigma = 2$–4 Å) were well fitted to the measured decay curves in the double-strand configurations. In the single-strand configurations, the results with good fits were obtained only when wide distribution widths were postulated ($\sigma = 10$–15 Å). Fig. 2 *B* shows distributions made using the obtained σ values of donor-acceptor distance in the single- and the double-strand configurations where 12 bases separate two fluorophores. In the case of $n = 4$ and $n = 8$ in the single-strand configurations and of $n = 4$ in the double-strand configuration, the decay curves showing good fits were not obtained when Gaussian functions were used for distance-distributions. The average distances estimated from quenching of Bodipy493/503 fluorescence in the spectra were 27.9 Å for $n = 4$ and 32.3 Å for $n = 8$ in the single strands and 32.2 Å for $n = 4$ in the double strands. In these close average distances, the distributions of the donor-acceptor should be largely different from the symmetric distributions, including the Gaussian, because it is nearly impossible that there are two fluorophores being stable within these close distances. The above results show that the measured decay curves are interpreted that distances between the donor and acceptor on the hybrids have wider distributions in the single-strand configurations than in the double-strand configurations. This explanation is consistent with the consideration that the single-strand part on the formed hybrid is structurally flexible whereas the double strand is relatively rigid.

The differences in donor decay curves between the single- and the double-strand configurations described above directly affect the acceptor decay curves, because the acceptor decay is convoluted with the decay curve of the paired donor. Indeed, as shown in Fig. 1, *C* and *F*, the fluorescence decay of Cy5 in the double-strand configurations was slower than the decay in the single-strand configurations.

Determination of the best mode of hybrid configurations for detection of hybrids

The signal-to-noise ratios for distinguishing Cy5 fluorescence due to FRET from Cy5 fluorescence due to direct excitation by light absorption are determined by two factors in changes in Cy5 fluorescence caused by hybrid formation. One factor is the delay of decay curve and another factor is enhancement of Cy5 fluorescence intensity. For better distinctions, the slower decay and the greater enhancement are desirable. However, these two factors are contradictory. As shown in Fig. 1, *A* and *D*, the enhancement of Cy5 fluorescence became greater when the number of nucleotides separating two fluorophores on the hybrid was smaller, which is caused by higher FRET efficiency. On the other hand, the decay curve became slower when the number of nucleotides (*n*) was larger. For finding the most desirable number of nucleotides (*n*) separating two fluorophores on the hybrid in the double- and the single-strand configurations, signal-to-noise ratios for distinguishing the decay curve in the hybrid from the decay curve of non-hybridizing oligonucleotides were estimated. The decay rate for each curve was estimated using the time window of 3–7 ns, and the deviation in the measurements was estimated from the fluorescence intensity within this time window (see Materials and Methods). Fig. 3 shows the estimated relative signal-to-noise ratios for distinguishing the decay curve in the hybrid from the decay curve of non-hybridizing oligonucleotides. The signal-to-noise ratios were higher in the double-strand configurations than in the single-strand configurations. The highest signal-to-noise ratio was obtained when the number of nucleotides (*n*) was 12 in the double-strand configuration, in which FRET efficiency was ~50%.

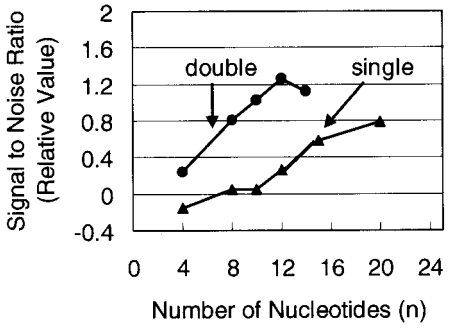

FIGURE 3 Distinguishing Cy5 fluorescence decay curves of hybridized oligonucleotides from Cy5 fluorescence decay curves of non-hybridizing oligonucleotides. The signal-to-noise ratios for distinguishing two decay curves were estimated as described in Materials and Methods.

In the experiments below for detection of target nucleic acids, we used a combination of two fluorescent oligonucleotides, which formed a hybrid with a target nucleic acid where 12 nucleotides separated the two fluorophores and there was no single-strand part.

Detection of target nucleic acids in the presence of excess amounts of non-hybridizing fluorescent oligonucleotides

To examine detection of a target DNA in the presence of excess amounts of fluorescent oligonucleotides, changes in Cy5 fluorescence decay curves were measured when the target DNA was added to the pair probe solutions (Fig. 4 *C*). Decay curves became slower as more target DNA was added, and these decay curves were clearly distinguishable even when the molar ratio of the target DNA to the pair fluorescent oligonucleotides was 1%. It was not distinguished in fluorescence decay curves of Bodipy493/503 (Fig. 4 *B*). Fluorescence spectral changes were also shown when the spatial separation between two fluorophores on the formed hybrid was 12 nucleotides ($n = 12$) and 4 nucleotides ($n = 4$) in Fig. 4, *A* and *D*, respectively. In $n = 4$, the largest spectral changes occur by hybrid formation. In these spectra, the distinction was actually less clear, in particular within the region where molar ratios of target DNA were low (1–5%). These results show that target DNA can be detected using Cy5 fluorescence decay curves under the condition that 100 times the number of non-hybridizing fluorescent oligonucleotides are present.

Detection of c-fos RNA

We applied the present method to detect c-fos RNA. The 657–696 sequence of human c-fos mRNA was used as a site for hybridization of oligonucleotides. The 657–696 site was highly accessible to oligonucleotides (Tsuji et al., 2000). The Bodipy493/503-labeled 20-mer DNA complementary to the 657–676 sequence and the Cy5-labeled 20-mer DNA complementary to the 677–696 sequence were used as a pair detection probe for c-fos RNA.

First, we measured fluorescence decay curves of Cy5 in DNA/RNA hybrids, using the 40-mer RNA having the 657–696 sequence of c-fos RNA as a target nucleic acid. Almost the same results were obtained as when the target nucleic acid was the 33-mer DNA (Fig. 4 *C*), although the decay curves were somewhat different (data not shown). These differences could be caused by differences in structural fluctuations of the formed hybrids between the DNA/DNA hybrids and the DNA/RNA hybrids.

Fig. 5 *A* shows fluorescence decay curves of Cy5 containing the pair fluorescent oligo-DNA probes and c-fos

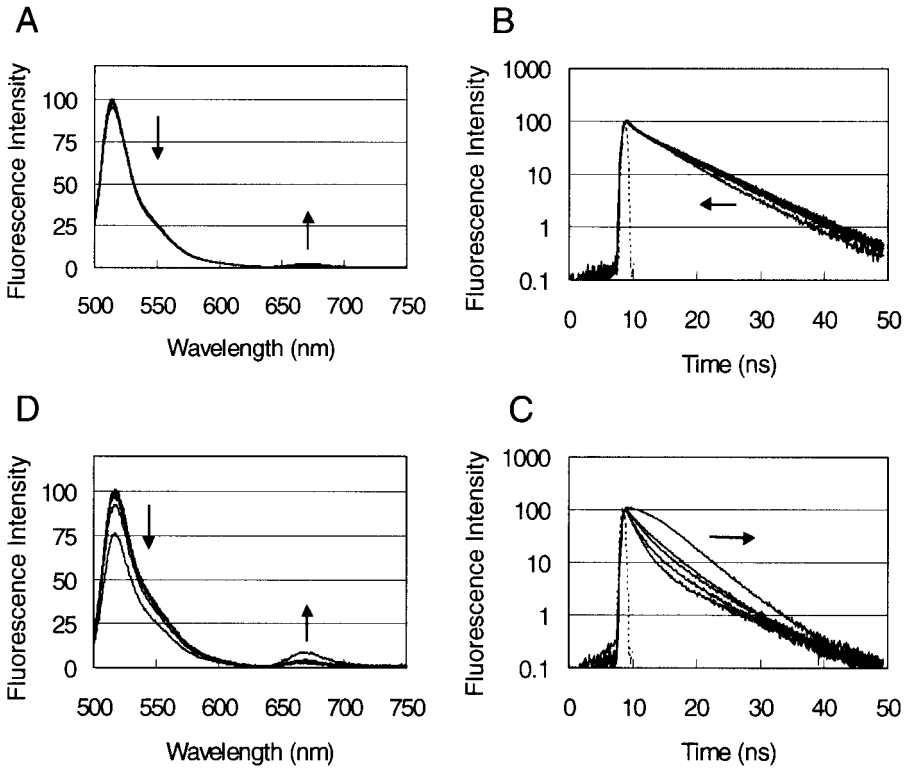

FIGURE 4 Detection of target DNA by measuring fluorescence decay curves of Cy5 in the presence of excess amounts of non-hybridizing fluorescent oligonucleotide probes. A pair of Bodipy493/503-labeled 16-mer DNA and Cy5-labeled 17-mer DNA was used as a probe for detection of the target 33-mer DNA. The pair fluorescent probes formed the hybrid with the target DNA where two fluorophores were separated by 12 nucleotides ($n = 12$) and there was double strand between two fluorophores. Spectra and decay curves of probe solution were measured, and then the target DNA was added sequentially to the probe solution in which the final molar ratios of the target DNA to probes were 1, 2.5, 5, and 20%. (*A*) Spectra. As c-fos RNA was added, fluorescence of Bidipy493/503 decreased and Cy5 fluorescence increased. (*B*) Decay curves of Bodipy493/503. As c-fos RNA was added, the decay became faster. The laser pulse measured by the streak scope is also shown as a broken line. (*C*) Decay curves of Cy5. As c-fos RNA was added, the decay became slower. (*D*) Changes in spectra when the pair fluorescent probes forming the hybrid where two fluorophores were separated by four nucleotides ($n = 4$) were used.

RNA at various molar ratios. c-fos RNA was synthesized by in vitro transcription reactions. As more c-fos RNA was added, the decays became slower. For evaluating changes in the decay curves, the fluorescence intensity in the time window of 0.5–1.5 ns ($I_{0.5–1.5}$) and that of 5.5–6.5 ns ($I_{5.5–6.5}$) after pulse excitation were used. Fig. 5 *B* shows the fluorescence intensity ratios ($I_{5.5–6.5}/I_{0.5–1.5}$) in decay curves of various molar ratios of c-fos RNA to the fluorescent oligo-DNA probes. The ratios ($I_{5.5–6.5}/I_{0.5–1.5}$) increased as more c-fos RNA were present. As a control experiment, xelf1-α RNA was added to the probe solution at a molar ratio of 20%. No change in the decay curve was observed (Fig. 5 *B*). These results show that c-fos RNA was specifically detected in the presence of excess amounts of non-hybridizing fluorescent oligonucleotides.

Specific detection of c-fos RNA in the presence of excess amounts of other kinds of mRNA

We examined the specificity of detection of c-fos RNA by measuring decay curves in the presence of excess amounts of other kinds of mRNA. For these experiments, we constructed a time-resolved fluorescence detection instrument of a gated counting method (see Materials and Methods). Two gated photomultipliers were placed in a T-format, and fluorescence from sample solutions was led to detectors through optical bandpass filters for Cy5 fluorescence. Fluorescence decay rate was estimated by the ratio of the fluorescence intensity in two time windows located at different times in the decay. In our gated counting measurements using two gated detectors, one time window was set at a fixed time and another window at various times. Using the gated detection in our instrument, changes in fluorescence decay were measured in low concentrations of fluorescent oligonucleotides (less than 10^{-8} M) within several seconds. (In measurements using the streak scope, a concentration of 10^{-6} M and several minutes for counting was needed for measurement of Cy5 fluorescence decay.)

Cy5 decay curves of mixtures of the pair fluorescent oligo-DNA probes and c-fos RNA with various molar ratios were obtained. For measurements of decay curves, the time window of 3-ns width was sequentially shifted at intervals

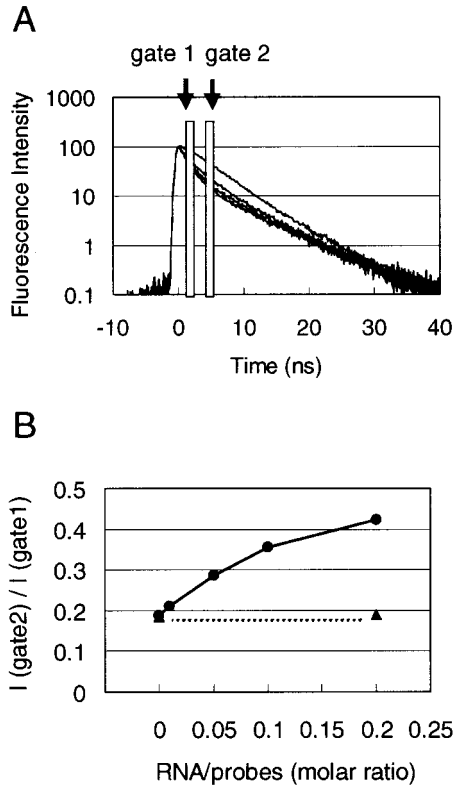

FIGURE 5 Detection of c-fos RNA. The 657–696 site of c-fos RNA was used as a hybridization site for the fluorescent oligo-DNA probes. The pair of fluorescent oligo-DNA probes and c-fos RNA were mixed at molar ratios of 1:0, 1:0.01, 1:0.05, and 1:0.2. (*A*) Decay curves of Cy5 fluorescence. (*B*) Fluorescence intensity in 0.5–1.5 ns (gate1) and in 5.5–6.5 ns (gate2) after pulse excitation was estimated, respectively, for each decay curve, and the ratios of fluorescence intensity ($I_{5.5-6.5}/I_{0.5-1.5}$) were plotted against the molar ratios of c-fos RNA to fluorescent oligo-DNA probes (●). As a control experiment, xelf1-α RNA was added to the probe solution, and the ratio value in the decay curve is also shown (▲).

of 1 ns. The obtained decay curves were almost the same as the decay curves measured by the streak scope shown in Fig. 5 *A*. For detection of changes in decay curves by hybrid formation of the pair fluorescent oligo-DNAs with c-fos RNA, the fluorescence intensity in the time window set at 0 ns after pulse excitation and that at 5 ns were used. The fluorescence intensity ratio values (I_{5ns}/I_{0ns}), which represent decay rates, were 0.21 for the probe solution, and 0.33, 0.43, 0.54, and 0.67 for the mixture solution in which the molar ratio of c-fos RNA to probes was 0.05, 0.1, 0.2, and 1.0, respectively.

When c-fos RNA was added to the probe solutions, in which final concentrations of c-fos RNA and probes were 10^{-8} M and 10^{-9} M, respectively, the time course of changes in the fluorescence ratio values (I_{5ns}/I_{0ns}) showed the hybrid formation occurred mostly within 30 min in this concentration. When polyA RNA extracted from NIH/3T3 cells was added to the fluorescent oligo-DNA probes for c-fos RNA, no change in I_{5ns}/I_{0ns} values was observed during 60 min (Table 3). Then, c-fos RNA was added to the solution for a molar ratio of 2.5% to the probes followed by 10%. The decays (I_{5ns}/I_{0ns}) changed in response to the presence of c-fos RNA whether or not there were excess amounts (2500-fold the weight of the 20-mer probe) of polyA RNA (Table 3). These results show that the present method can detect a specific RNA among excess amounts of non-hybridizing fluorescent oligonucleotide probes and other kinds of mRNA.

Time-resolved microscopy

To apply the time-resolved measurement method to observe hybrid in a single living cell under a microscope, we constructed a time-resolved fluorescence microscope equipped with cooled CCD cameras with a time-gate function (Fig. 6). As in the measurements in the gated counting method using gated photomultipliers described above, the time window for the first camera was set at a fixed time on the decay curve and that for the second camera at another time, and ratio images of fluorescence intensity in the two time windows were obtained.

Fig. 7 *A* shows Cy5 fluorescence decay curves obtained in the time-resolved fluorescence microscope. Fluorescent oligonucleotide pair probes and target 40-mer DNA were mixed with various molar ratios and each solution was dropped on coverslips. The time window of the first camera was located at 0 ns after pulse excitation, and the locations of the time window for the second camera were varied from −1 ns to 13 ns. Gate width was 5 ns for both cameras. The obtained decay curves were almost the same as those measured using gated photomultipliers (The curves obtained were broader than those measured by photomultipliers, because of the broader gate width in the cameras). Fig. 7 *A* also shows the decay curve of autofluorescence of a Hela cell. The decay was faster than the Cy5 fluorescence decay of probes. When the gate for the second camera was set at

TABLE 3 Detection of c-fos RNA in the presence of excess amounts of other kinds of polyA RNA

Oligonucleotide probes (1×10^{-8} M)	c-fos RNA (1×10^{-8} M)	polyA RNA (1×10^{-8} M)	I_{5ns}/I_{0ns}
1	0	0	0.22
1	0	1	0.21
1	0	30	0.22
1	0.025	30	0.30
1	0.1	30	0.44
1	0.025	0	0.31
1	0.1	0	0.44

Concentrations of c-fos RNA and polyA RNA were estimated from absorbance at 260 nm as 1 absorbance to 35 μg. Added amounts of polyA RNA were 80-fold and 2500-fold weight of the 20-mer probes, respectively. For estimation of mole concentrations, the average nucleotide numbers of polyA RNA was postulated as 1500. Each measurement was performed at 60 min after addition of RNA.

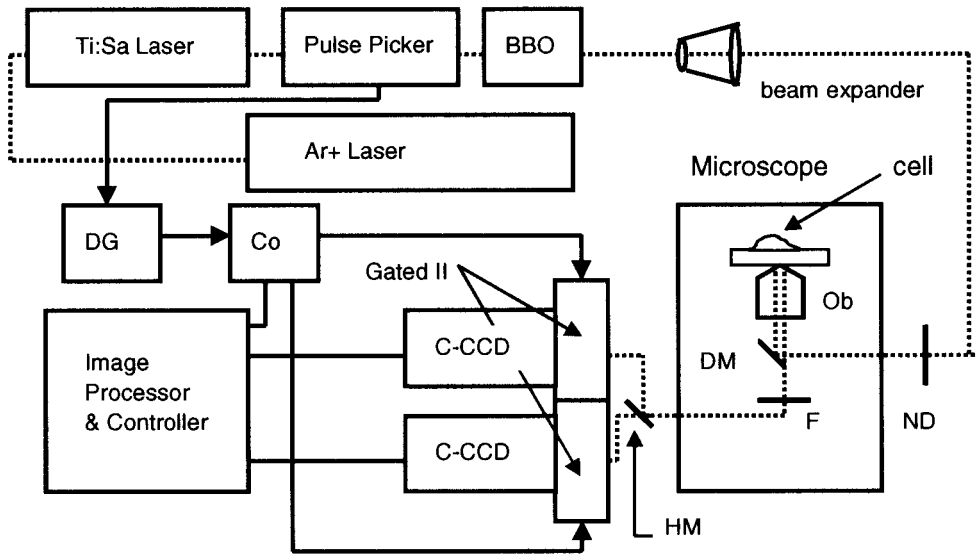

FIGURE 6 Block diagram of time-resolved fluorescence microscope. DG, delay generator; Co, Gated II controller; ND, neutral density filter; Ob, objective; DM, dichroic mirror; F, barrier filter; HM, half mirror; Gated II, image intensifier with time-gate function; C-CCD; cooled CCD camera.

5 ns, ratio values of cell autofluorescence, probe solution, and hybrid solution were 0.24, 0.38, and 1.21, respectively.

Detection of hybrid in living cells

We examined the extent of interference of cell autofluorescence in detection of hybrid in living cells by injecting various concentrations of hybrid solutions or probe solutions into the cytoplasm of Hela cells and obtaining fluorescence ratio images of the injected cells for detecting FRET signals in the cytoplasm.

Fig. 8 shows results in the conventional microscope. For detecting FRET, both donor fluorescence image (DD) and acceptor fluorescence image (DA) with donor excitation were acquired, and the ratio image (DA/DD) was obtained. In the ratio image, the ratio value was estimated in each pixel, and then the distribution pattern of ratio values in the whole cytoplasm was obtained. Each line in columns of Figs. 8 and 9 shows the distribution of fluorescence ratio values in each cell. First, we injected 1×10^{-5} M of probe solution or hybrid solution. On the hybrid, donor and acceptor were separated by four nucleotides. If we assume that the cell volume is 1.5×10^{-12} L and the injected volume is 1% of the cell volume, there were ~90,000 molecules in the cytoplasm. Fig. 8, *b* and *d*, shows ratio value distributions in cells injected with probe solution and hybrid solution, respectively. In probe-injected cells, the ratio values had distributions centered at 0.18 with 0.10 of half-width (Fig. 8 *b*). When hybrids were injected, the ratio values were distributed around 2.0 with broader distributions (0.71 of half-width) than that of probes (Fig. 8 *d*). These ratio values (0.18 for probes and 2.0 for hybrids) were almost the same as the values of the respective solutions on coverslips (Tsuji et al., 2000). Ratio value distributions in non-injected cells (cell autofluorescence) are also shown (Fig. 8 *a*). In the cells injected with ~90,000 molecules of oligonucleotide probes, fluorescence intensity of oligonucleotide probes is enough higher than cell autofluorescence intensity in both DD and DA images to estimate ratio values accurately for FRET detection. Injected hybrids were not homogeneously distributed throughout the cytoplasm within 5 min after injection. In the region where there were relatively small numbers of hybrids, cell autofluorescence intensity was not negligible compared with the fluorescence from hybrids, especially in DD images. (Cell autofluorescence is stronger in DD images than in DA images, because the wavelength in measurements is separated less from the excitation wavelength in DD images.) That reduced ratio values in these regions and made the broader distribution.

When the numbers of injected molecules decreased, cell autofluorescence intensity became comparable to or stronger than fluorescence intensity of oligonucleotide probes throughout the cytoplasm, especially in DD images, and interference of cell autofluorescence in measurements of ratio values became larger. Fig. 8, *c* and *e*, shows the results of injection of 1×10^{-6} M probes and 5×10^{-7} M hybrids, respectively. In these cells, it became impossible to distinguish the ratio value distributions of probe-injected cells or hybrid-injected cells from the distribution pattern of cell autofluorescence, which means hybrids cannot be detected.

The same experiments were performed under the time-resolved microscope (Fig. 9). Results from injection of 1×10^{-5} M probe solution and hybrid solution are shown in Fig. 9, *b* and *d*, respectively. On the hybrid, donor and acceptor were separated by 12 nucleotides. Fluorescence images of these cells are shown in Fig. 7 *B*. When probe

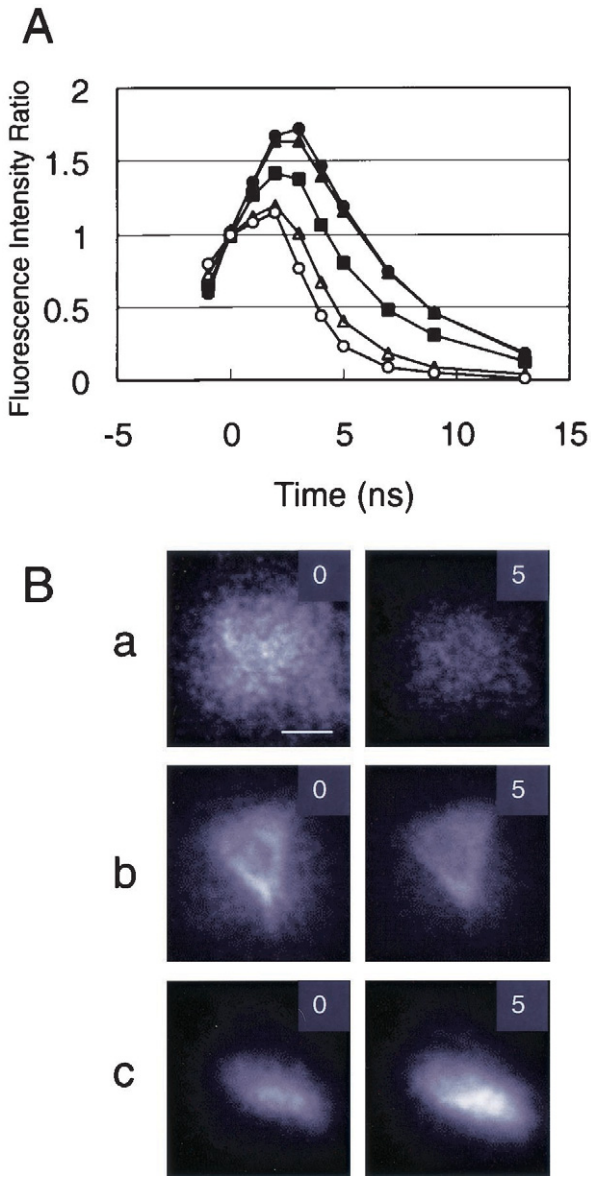

FIGURE 7 (*A*) Cy5 fluorescence decay curves obtained in the time-resolved microscope. The oligo-DNA pair probes were mixed with the target 40-mer DNA at various molar ratios and the solution (1×10^{-6} M) was dropped on coverslips. The time window (5-ns width) for the first camera was set at 0 ns after pulse excitations, and the locations of the second camera time windows were varied from −1 ns to 13 ns. Fluorescence images were measured and the ratio of fluorescence intensity in the second camera image to that in the first camera image was estimated. Molar ratios of target DNA to probes were 0 (probe solution; △), 0.1 (■), 0.2 (▲), and 1.0 (●). Decay of Hela cell autofluorescence was also measured (○). (*B*) Cy5 fluorescence images of Hela cells obtained in the time-resolved microscope. The time windows were set at 0 ns after pulse excitation for the first camera and at 5 ns for the second camera. The first camera images (0) and the second camera images (5) are shown. (*a*) Cell autofluorescence; (*b*) 1×10^{-5} M probe solutions were injected; (*c*) 1×10^{-5} M hybrid solutions were injected. The images are shown in different bit ranges: 1–8 (*a*), 3–10 (*b*), and 4–11 (*c*). Bar, 20 μm

solutions were injected into the cytoplasm of Hela cells, the ratio values representing acceptor fluorescence decay rates were distributed around 0.29 with 0.07 of half-width. When hybrid solutions were injected, ratio values were distributed broadly (as in the case of measurements in the conventional microscope) from 0.5 to 1.5. The average ratio value of cell autofluorescence having faster decays was 0.24 (0.05 of half-width; *a*). As the numbers of injected molecules decreased, acceptor fluorescence intensity in the cytoplasm decreased and then measured decay curves became the mixture of acceptor fluorescence decay and cell autofluorescence decay. As a result, the obtained ratio values decreased toward the values of cell autofluorescence (Fig. 9, *c* and *e*). In measurements under the time-resolved microscope, detection of hybrids was possible when 1×10^{-7} M hybrid solution was injected (~900 molecules were present throughout the cytoplasm).

The difference in detection limit of hybrids between conventional microscopy (spectral measurements) and time-resolved microscopy mainly arises from cell autofluorescence. To measure FRET quantitatively using fluorescence spectra, measurements of donor fluorescence as well as acceptor fluorescence are required. On the other hand, only acceptor fluorescence is measured in the time-resolved method we used in this study. Interference of cell autofluorescence in measurements of fluorescence signals is larger in the region of donor fluorescence wavelength than in the region of acceptor fluorescence. In addition, decay of cell autofluorescence ends within 1 ns in most cases, which is faster than decays of fluorophores. That also helps to distinguish fluorophore fluorescence from cell autofluorescence.

General Discussion

We demonstrated that FRET signals in the presence of excess amounts of non-FRET fluorescence molecules are detected using the time-resolved measurements of acceptor fluorescence decays. Measurements of acceptor decays are also demonstrated to be useful for detecting FRET signals in the presence of cell autofluorescence in living cells. The cell autofluorescence intensity decreases because of large separation of the measurement wavelength from the excitation wavelength and FRET signals are distinguished from cell autofluorescence by differences in decay rates. In this study, we used a combination of Bodipy493/503 and Cy5 as a donor and an acceptor, which has a seven times longer difference in fluorescence lifetime. If a fluorophore having the longer fluorescence lifetime is used as a donor, the signal-to-noise ratios for distinguishing the FRET fluorescence from the non-FRET fluorescence and cell autofluorescence will increase more.

FRET has been also used recently as a tool to detect associations of proteins and protein conformational

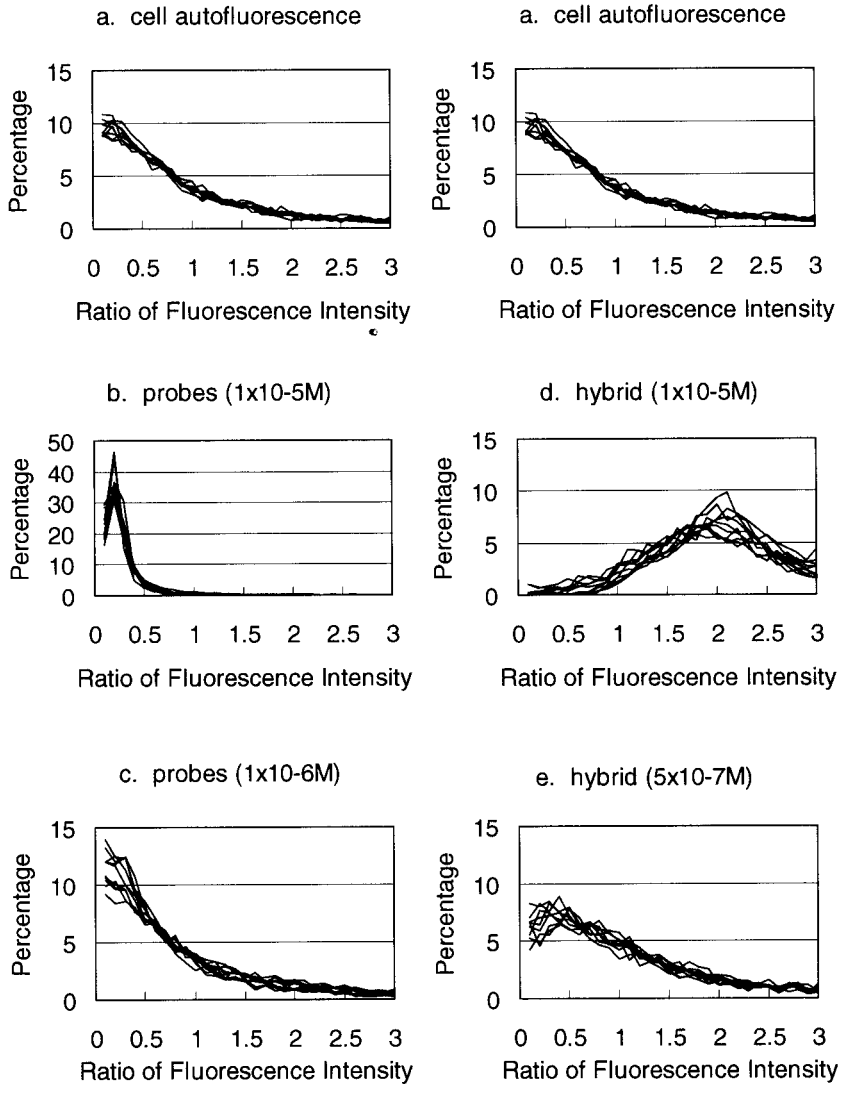

FIGURE 8 Fluorescence imaging detection of hybrid in the cytoplasm of Hela cells in the conventional microscope. Probe solutions or hybrid solutions were injected into the cytoplasm of Hela cells, and fluorescence ratio images of the cells were obtained in the conventional fluorescence microscope. Each line in columns shows the distribution of ratio values in the whole cytoplasm of the cell. (*a*) Non-injected cells (autofluorescence); (*b*) 1×10^{-5} M probe; (*c*) 1×10^{-6} M probe; (*d*) 1×10^{-5} M hybrid; (*e*) 5×10^{-7} M hybrid. On the hybrid, donor and acceptor were separated by four nucleotides.

changes in living cells (Tsien et al., 1993; Bastiaens and Squire, 1999; Day et al., 1999). In these studies, FRET was measured under a microscope by obtaining images of donor fluorescence intensity and acceptor fluorescence intensity (Miyawaki et al., 1997; Mahajan et al., 1998) or by using donor fluorescence decays (Gadella and Jovin, 1995; Ng et al., 1999; Verveer et al., 2000). Use of acceptor decays for measurements of FRET will improve signal-to-noise ratios for detecting FRET in the presence of excess amounts of non-FRET fluorescence molecules and in the presence of cell autofluorescence and make it possible to detect small numbers of fluorescence molecules participating in FRET in living cells. To make acceptor decays become slower, a narrow distance-distribution of donor and acceptor is preferable. Specific labeling of fluorophores to the proteins rigidly will minimize fluctuations in distance, and there will be relatively small fluctuations of fluorophores when proteins are tagged with green fluorescent protein.

We previously reported that c-fos mRNA was observed in living Cos7 cells under a conventional fluorescence microscope when c-fos mRNA was expressed at more than 10^4 molecules in a cell (Tsuji et al., 2000). The present method will be useful for detecting small numbers of mRNA. Taking images of induced expressions of c-fos mRNA is currently under study.

We thank Masayo Takayanagi for her excellent technical assistance.

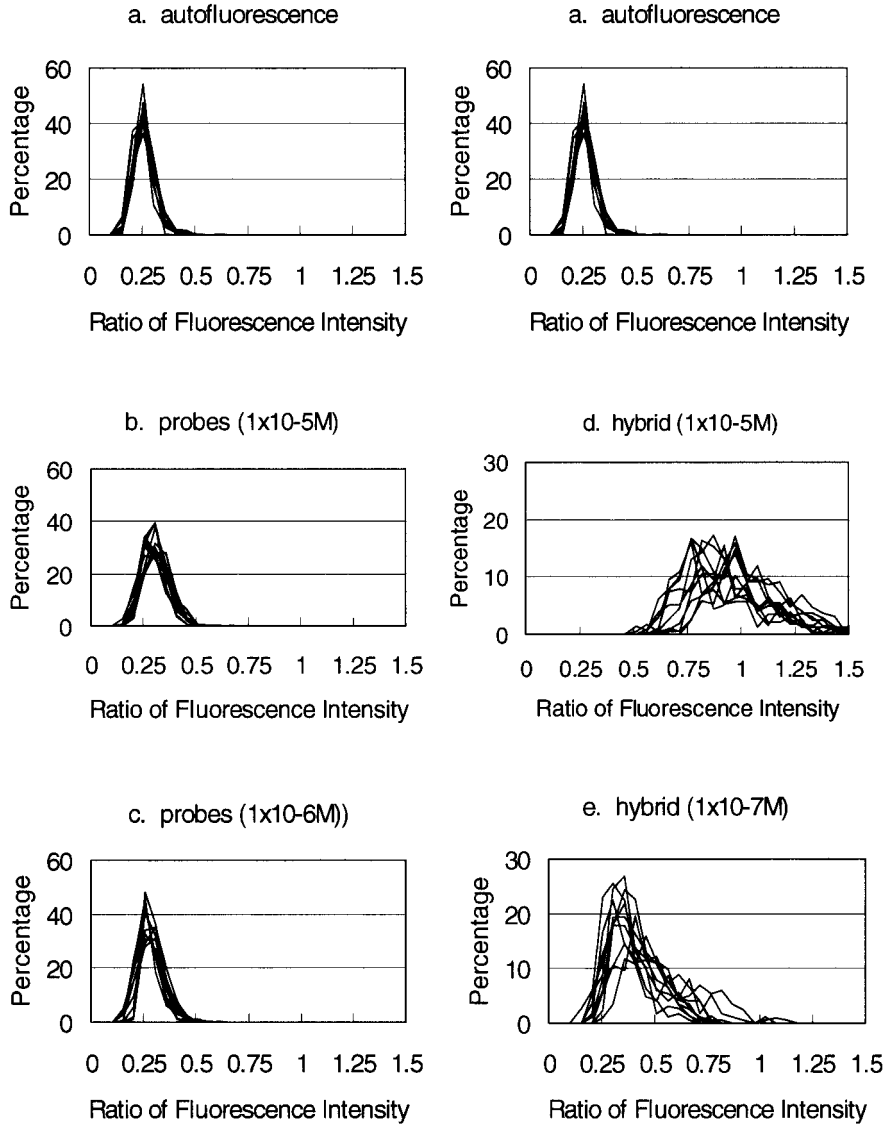

FIGURE 9 Fluorescence imaging detection of hybrid in the cytoplasm of Hela cells in the time-resolved microscope. Probe solutions or hybrid solutions were injected into the cytoplasm of Hela cells and fluorescence ratio images of the cells were obtained in the time-resolved microscope. Each line in columns shows the distribution of ratio values in whole cytoplasm of the cell. (*a*) Non-injected cells (autofluorescence); (*b*) 1×10^{-5} M probe; (*c*) 1×10^{-6} M probe; (*d*) 1×10^{-5} M hybrid; (*e*) 1×10^{-7} M hybrid. On the hybrid, donor and acceptor were separated by 12 nucleotides.

REFERENCES

Axelrod, D. 1989. Total internal reflection fluorescence microscopy. *Methods Cell Biol.* 30:245–270.

Bastiaens, P. I. H., and A. Squire. 1999. Fluorescence lifetime imaging microscopy: spatial resolution of biochemical processes in the cell. *Trends Cell Biol.* 9:48–52.

Cardullo, R. A., S. Agrawal, C. Flores, P. C. Zamecnik, and D. E. Wolf. 1988. Detection of nucleic acid hybridization by nonradiative fluorescence resonance energy transfer. *Proc. Natl. Acad. Sci. U.S.A.* 85: 8790–8794.

Clegg, R. M., A. I. H. Murchie, A. Zechel, and D. M. Lilley. 1993. Observing the helical geometry of double-stranded DNA in solution by fluorescence resonance energy transfer. *Proc. Natl. Acad. Sci. U.S.A.* 90:2994–2998.

Day, R. N., S. K. Nordeen, and Y. Wan. 1999. Visualizing protein-protein interactions in the nucleus of the living cells. *Mol. Endocrinol.* 13: 517–526.

Eis, P. S., and J. R. Lakowicz. 1993. Time-resolved energy transfer measurements of donor-acceptor distance distributions and intramolecular flexibility of CCCH zinc finger peptides. *Biochemistry.* 32: 7981–7993.

Gadella, T. W. J., Jr., and T. M. Jovin. 1995. Oligomerization of epidermal growth factor receptors on A431 cells studied by time-resolved fluorescence imaging microscopy: a stereochemical model for tyrosine kinase receptor activation. *J. Cell Biol.* 129:1543–1558.

Grinvald, A., E. Haas, and I. Z. Steinberg. 1972. Evaluation of the distribution of distances between energy donors and acceptors by fluorescence decay. *Proc. Natl. Acad. Sci. U.S.A.* 69:2273–2277.

Haran, G., E. Haas, B. K. Szpikowska, and M. T. Mas. 1992. Domain motions in phosphoglycerate kinase: determination of interdomain distance distribution by site-specific labeling and time-resolved fluorescence energy transfer. *Proc. Natl. Acad. Sci. U.S.A.* 89:11764–11768.

Mahajan, N. P., K. Linder, G. Berry, G. W. Gordon, R. Heim, and B. Herman. 1998. Bcl-2 and Bax interactions in mitochondria probed with

green fluorescent protein and fluorescence resonance energy transfer. *Nat. Biotechnol.* 16:547–552.

Mergny, J-L., A. S. Boutorine, T. Garestier, F. Belloc, M. Rougee, N. V. Bulychev, A. A. Koshkin, J. Bourson, A. V. Lebedev, B. Valeur, N. T. Thung, and C. Helene. 1994. Fluorescence energy transfer as a probe for nucleic acid structures and sequences. *Nucleic Acids Res.* 22:920–928.

Miyawaki, A., J. Llopis, R. Heim, J. M. McCaffery, J. A. Adams, M. Ikura, and R. Tsien. 1997. Fluorescent indicators for Ca^{2+} based on green fluorescent proteins and calmodulin. *Nature.* 388:882–887.

Morrison, L. E. 1988. Time-resolved detection of energy transfer: theory and application to immunoassays. *Anal. Biochem.* 174:101–120.

Ng, T., A. Squire, G. Hansra, F. Bornacin, C. Prevostel, A. Hanby, W. Harris, D. Barnes, S. Schmidt, H. Mellor, P. I. H. Bastiaens, and P. J. Parker. 1999. Imaging protein kinases Cα activation in cells. *Science.* 283:2085–2089.

Parkhurust, K. M., and L. J. Parkhurust. 1995. Donor-acceptor distance distributions in a double-labeled fluorescent oligonucleotide both as a single strand and in duplexes. *Biochemistry.* 34:293–300.

Sako, Y., S. Minoghchi, and T. Yanagida. 2000. Single-molecule imaging of EGFR signaling on the surface of living cells. *Nat. Cell Biol.* 2:168–172.

Sei-Iida, Y., H. Koshimoto, S. Kondo, and A. Tsuji. 2000. Real-time monitoring of in vitro transcriptional RNA synthesis using fluorescence resonance energy transfer. *Nucleic Acids Res.* 28:e59.

Soper, S. A., B. L. Legender, Jr., and D. C. Williams. 1995. On-line fluorescence lifetime determinations in capillary electrophoresis. *Anal. Chem.* 67:4358–4365.

Sixou, S., F. C. Szoka, Jr., G. A. Green, B. Giusti, G. Zon, and D. J. Chin. 1994. Intracellular oligonucleotide hybridization detected by fluorescence resonance energy transfer (FRET). *Nucleic Acids Res.* 22: 662–668.

Tsien, R. Y., B. J. Bacskai, and S. R. Adams. 1993. FRET for studying intracellular signalling. *Trends Cell Biol.* 3:242–245.

Tokunaga, M., K. Kitamura, K. Saito, A. Iwane, and T. Yanagida. 1997. Single molecule imaging of fluorophores and enzymatic reactions achieved by objective-type total internal reflection fluorescence microscopy. *Biochem. Biophys. Res. Commun.* 235:47–53.

Tsuji, A., H. Koshimoto, Y. Sato, M. Hirano, Y. Sei-Iida, S. Kondo, and K. Ishibashi. 2000. Direct observation of specific messenger RNA in a single living cell under a fluorescence microscope. *Biophys. J.* 78: 3260–3274.

Verveer, P. J., F. S. Wouters, A. R. Reynolds, and P. I. H. Bastiaens. 2000. Quantitative imaging of lateral ErbB1 receptor signal propagation in the plasma membrane. *Science.* 290:1567–1570.